

The quasar fraction in low-frequency selected complete samples and implications for unified schemes

Chris J. Willott^{1,2*}, Steve Rawlings¹, Katherine M. Blundell¹ and Mark Lacy^{1,3}

¹ Astrophysics, Department of Physics, Keble Road, Oxford, OX1 3RH, U.K.

² Instituto de Astrofísica de Canarias, C/ Via Lactea s/n, 38200 La Laguna, Tenerife, Spain

³ IGPP, L-413, Lawrence Livermore National Laboratory, Livermore, CA 94550, USA

25 October 2018

ABSTRACT

Low-frequency radio surveys are ideal for selecting orientation-independent samples of extragalactic sources because the sample members are selected by virtue of their isotropic steep-spectrum extended emission. We use the new 7C Redshift Survey along with the brighter 3CRR and 6C samples to investigate the fraction of objects with observed broad emission lines – the ‘quasar fraction’ – as a function of redshift and of radio and narrow emission line luminosity. We find that the quasar fraction is more strongly dependent upon luminosity (both narrow line and radio) than it is on redshift. Above a narrow [OII] emission line luminosity of $\log_{10}(L_{\text{[OII]}}/\text{W}) \gtrsim 35$ [or radio luminosity $\log_{10}(L_{151}/\text{W Hz}^{-1} \text{ sr}^{-1}) \gtrsim 26.5$], the quasar fraction is virtually independent of redshift and luminosity; this is consistent with a simple unified scheme with an obscuring torus with a half-opening angle $\theta_{\text{trans}} \approx 53^\circ$. For objects with less luminous narrow lines, the quasar fraction is lower. We show that this is not due to the difficulty of detecting lower-luminosity broad emission lines in a less luminous, but otherwise similar, quasar population. We discuss evidence which supports at least two probable physical causes for the drop in quasar fraction at low luminosity: (i) a gradual decrease in θ_{trans} and/or a gradual increase in the fraction of lightly-reddened ($0 \lesssim A_V \lesssim 5$) lines-of-sight with decreasing quasar luminosity; and (ii) the emergence of a distinct second population of low luminosity radio sources which, like M87, lack a well-fed quasar nucleus and may well lack a thick obscuring torus.

Key words: galaxies: active – galaxies: nuclei – quasars: general – galaxies: evolution

1 INTRODUCTION

Orientation-based unified schemes for radio-loud quasars and powerful radio galaxies play a key role in our understanding of these objects. Ever since the conception of the idea that powerful radio galaxies are simply quasars with their jet axes oriented away from our line of sight, such that the nuclear continuum and broad-line regions are obscured by a dusty torus or warped disc (Scheuer 1987; Barthel 1989), evidence has been sought to prove that these unification schemes are correct. Reviews of unification schemes for active galactic nuclei have been presented by Antonucci (1993) and Urry & Padovani (1995). Although the majority of observations are consistent with them, some observations

have been used to cast doubt on their viability over all ranges of radio luminosities and redshifts.

The narrow line emission in radio sources is observed to be emitted largely from beyond the obscuring material (e.g. McCarthy, Spinrad & van Breugel 1995; Hes, Barthel & Fosbury 1996) and therefore is independent of the jet axis orientation. Hence in this model one would expect radio galaxies and quasars to have similar narrow line luminosities. The strong positive correlation between the extended radio luminosities and narrow line luminosities of radio sources (Baum & Heckman 1989; Rawlings et al. 1989; Willott et al. 1999) means that the samples of radio galaxies and quasars to be compared must be matched in extended radio luminosity. At low redshift ($z < 0.8$), there have been claims that quasars are observed to have [OIII] line luminosities a factor of 5–10 greater than radio galaxies of similar radio luminosities (Baum & Heckman 1989; Jackson & Browne 1990; Lawrence 1991), although the [OII] luminosities of radio galaxies and

* Email: cjh@astro.ox.ac.uk

quasars at these redshifts are indistinguishable (Browne & Jackson 1992; Hes et al. 1996). These differences between [OII] and [OIII] have been interpreted as being due to partial obscuration of [OIII] since its higher ionization potential means it is likely to be emitted from closer to the nucleus than [OII]. However, Jackson & Rawlings (1997) have investigated the [OIII] luminosities of $z > 1$ radio galaxies and quasars and find their distributions indistinguishable. Using a combined 7C/3CRR dataset Willott et al. (1999) find that quasars have more luminous narrow lines than radio galaxies at intermediate radio luminosities [$26 < \log_{10}(L_{151} / \text{W Hz}^{-1}\text{sr}^{-1}) < 27$], but they are similar at higher radio luminosities; this result leads to different slopes for the narrow-line versus radio luminosity correlation for quasars and radio galaxies.

Barthel (1989) showed that in the redshift range $0.5 < z < 1.0$ the linear size distributions and fraction of quasars in the 3CRR sample are consistent with all radio galaxies having their jet axes at an angle $\theta_{\text{trans}} > 44^\circ$ from our line-of-sight and all the quasars having $\theta_{\text{trans}} < 44^\circ$, where θ_{trans} is the half-opening angle of the obscuring torus; a value of $\theta_{\text{trans}} = 45^\circ$ has been adopted by many on the basis of this paper. However, at higher redshifts in the 3CRR sample, the fraction of quasars increases giving $\theta_{\text{trans}} \approx 60^\circ$ (e.g. Singal 1993). Note that because of the tight luminosity-redshift correlation inherent in a single flux-limited sample, this apparent correlation with redshift may be due instead to a correlation with radio luminosity. Singal (1996) used several large samples with differing radio flux-density limits to find that the quasar fraction in radio samples declines with decreasing radio flux-densities. However, due to the correlation between the optical and radio luminosities of steep-spectrum quasars (Serjeant et al. 1998; Willott et al. 1998a), radio-fainter samples will contain optically-fainter quasars. Therefore the quasar fraction in faint samples might be underestimated if only quasars brighter than a certain optical magnitude limit are identified, which may well be the case in some of these fainter samples used by Singal.

Using the new 7C Redshift Survey, a low-frequency radio sample selected at a flux-density limit $25\times$ lower than the 3CRR sample with $\approx 90\%$ spectroscopic redshift completeness, we have previously shown that the quasar fraction does not depend strongly upon radio luminosity or redshift for $1 < z < 3$ (Willott et al. 1998b). Note that the low-frequency selection of the samples is crucial, because this ensures selection on *extended* radio flux which should be entirely isotropic. In this paper we use a larger sample to investigate how the quasar fraction of radio sources depends upon redshift, radio luminosity and narrow emission line luminosity and we consider the implications for orientation-based unified schemes. In a companion paper (Blundell, Rawlings & Willott in prep.) we will investigate the constraints placed on unified schemes by the radio properties of quasars and radio galaxies from the combined 7C/6C/3CRR dataset. We assume throughout this paper that $H_0 = 50 \text{ km s}^{-1}\text{Mpc}^{-1}$ and $q_0 = 0.5$.

2 THE SAMPLE

Our sample consists of three completely-identified samples selected at (similar) low radio frequencies. These samples

have different flux limits to provide broad coverage of the radio luminosity-redshift ($L_{151} - z$) plane (see Figure 1). This enables the separation of evolutionary- and luminosity-dependent effects.

Our faintest sample is the 7C Redshift Survey which is briefly described here (see also Willott et al. 1998a; Willott et al. in prep.; Blundell et al. in prep; Lacy et al. 1999). The 7C Redshift Survey includes all sources with flux-densities at 151 MHz $S_{151} \geq 0.5 \text{ Jy}$ in three selected regions of sky (7C-I, 7C-II and 7C-III with a total sky area of 0.022 sr). The sample contains 130 radio sources which have all been identified with an optical/near-IR counterpart. The spectroscopic completeness is $\approx 90\%$ with most of the remaining sources having redshifts well-constrained by optical/near-IR photometry (Willott, Rawlings & Blundell, in prep.).

The bright sample used is the 3CRR sample of Laing, Riley & Longair (1983), which has complete redshift information for all 173 sources, selected with $S_{178} \geq 10.9 \text{ Jy}$. 3C 231 (M82) is excluded because it is a nearby starburst galaxy and not a radio-loud AGN. 3C 345 and 3C 454.3 are flat-spectrum quasars which are excluded on the grounds of Doppler-boosting of compact components being responsible for raising their fluxes above the selection limit. One quasar from the 7C sample (5C7.230) was excluded for the same reason.

The intermediate flux-density sample used is a revision of the 6C sample of Eales (1985) (see Rawlings, Eales & Lacy in prep., hereafter REL, for details). The flux limits of this sample are $2.0 \leq S_{151} < 3.93 \text{ Jy}$ and the sky area covered is 0.103 sr. Only 2 of the 58 sources in this sample do not have redshifts determined from spectroscopy. One object is faint in the near-infrared ($K > 19$), so we take it as a galaxy at $z = 2.0$ in this paper. The other is relatively bright in the near-IR but very faint in the optical. Its red colour suggests a galaxy with a redshift in the range $0.8 < z < 2$ and we assume $z = 1.4$ here. Full details of the sample, including optical spectra, will appear in REL.

All the sources in two of the three 7C regions, 7C-I and 7C-II, and in the 6C sample have been imaged in the near-infrared K -band. This has enabled the discovery of a few lightly reddened quasars, which would otherwise have been identified as galaxies on the basis of optical spectroscopy (see e.g. Willott et al. 1998a). In addition we have obtained near-infrared spectroscopy of some possible reddened quasars in these samples to search for broad emission lines (Willott et al. in prep.). On the basis of the available imaging and spectroscopy, all sources have been classified into one of three categories: quasar, broad line radio galaxy (BLRG) or radio galaxy. Given the relatively small number of reddened quasars found in the 6C, 7C-I and 7C-II samples, we do not believe the lack of near-infrared data for the 7C-III sample has caused a statistically-significant number of quasars to be mis-classified. Spectra of the quasars and BLRGs in 7C-I and 7C-II are presented with a detailed discussion of the classification scheme in Willott et al. (1998a).

Our total sample comprises 356 sources (one object, 3C 200, is common to both the 3CRR and 7C-II samples). We do not exclude compact symmetric objects (CSOs) from our analysis as previous authors have (e.g. Barthel 1989, Singal 1996), since we have no a priori reason to expect them not to be part of the unified schemes. In Section 3 we repeat our analysis excluding the CSOs to check this assumption.

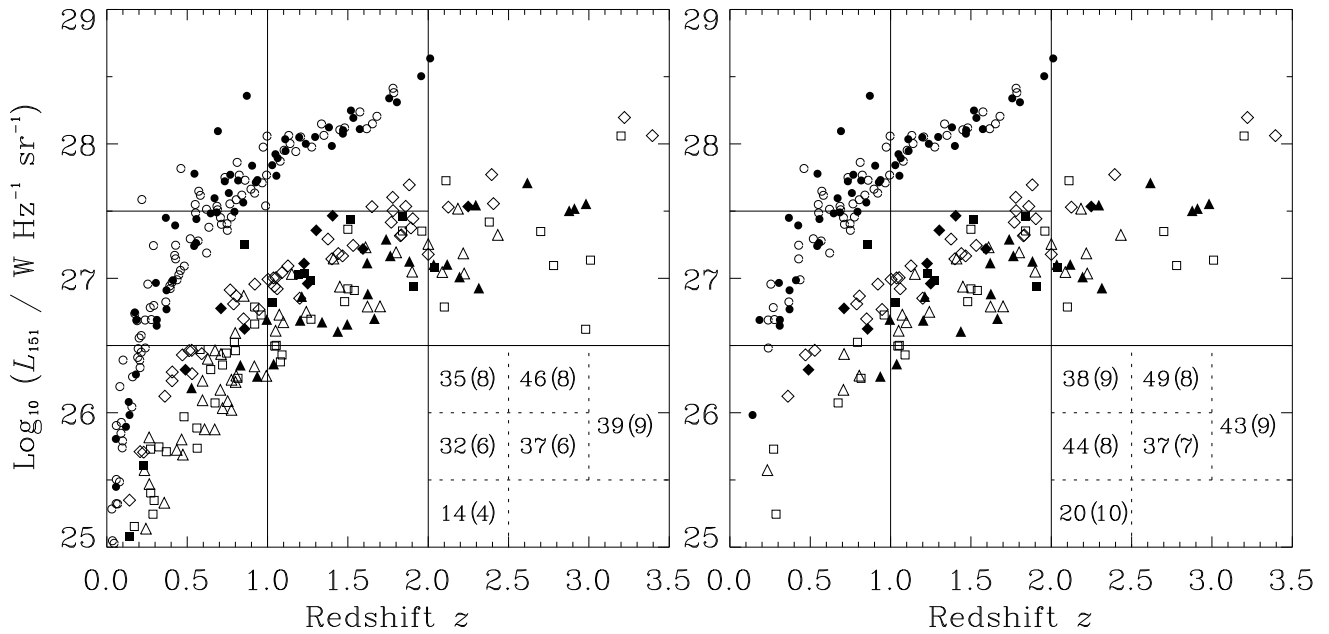


Figure 1. The radio luminosity–redshift plane for the 3CRR (circles), 6C (diamonds), 7C-I and 7C-II (triangles) and 7C-III (squares) complete samples in which only the 323 objects deemed FRIIs are plotted (see Section 2). Filled symbols are quasars or broad line radio galaxies and open symbols are radio galaxies. We have binned the $L_{151} - z$ plane in luminosity and redshift, of which 6 bins are well populated by sources from the complete samples. The percentage of quasars along with associated Poisson errors in each bin are shown in the bottom-right corner of the plot. The left plot shows all the FRII sources in the complete samples, whereas the right plot shows only those in the high emission-line luminosity category (see text for details). Note that there is one additional radio galaxy in the 7C-III sample which may be at $z > 4$ (Lacy et al. 1999).

Sources with FRI radio structure are however excluded. The main reason for this was a practical one: most (24 out of 33) of the FRIs are from the 3CRR sample, and the existing spectrophotometry of these objects is inadequate for the quantitative investigations of this paper. However, as discussed fully in Section 4.5, the lack of quasars with FRI radio structure (e.g. Falcke, Gopal-Krishna & Biermann 1995), and the concentration of these objects at low L_{151} and low z (see Fig. 1) makes it easy to investigate the effects of the exclusion of FRIs on our study of the quasar fraction. Although the radio structures of the quasars 5C6.264 and 3C 48 are arguably FRI, we count them in this paper as FRIIs because of their high radio luminosities. Indeed all objects that could not unambiguously characterised as FRI or FRII (e.g. the ‘DA’ sources in the notation of Blundell et al. in prep.) are also counted as FRIIs in this study. Thus our total combined sample contains 323 objects deemed to be FRIIs.

3 THE QUASAR FRACTION

We now investigate the fraction of objects which show broad emission lines (referred to hereafter simply as the quasar fraction) in the complete radio samples. Broad line radio galaxies (broad line objects with $M_B > -23$) are counted as quasars in this analysis, because they are most likely to be weak quasars viewed within the torus opening angle (Laing et al. 1994; Hardcastle et al. 1998; Fig. 6 of Willott et al. 1998a). However, objects with scattered broad lines

seen only in polarised light (4 cases) are counted as galaxies, because the fact that the broad lines are not observed directly indicates that the nuclear regions are heavily obscured, most likely by the torus. Since spectropolarimetry is unavailable for most sources, there is clearly some danger that the split between weak and scattered-light quasars is imperfect. A further concern is the question of the classification of lightly-reddened broad-line objects in which it remains uncertain whether (a) the reddening is related to the torus or is caused by dust further from the nucleus, for example in the host galaxy of the quasar; and (b) whether, particularly given the inhomogeneous spectrophotometric dataset for the 3CRR sample, all such objects have yet to be discovered. Taking $0 \lesssim A_V \lesssim 5$ as a working definition of ‘light’ reddening, we have chosen to count all such objects known to us as quasars. We will return to this important point in Section 4.2.

In Fig. 1 (left), we plot low-frequency radio luminosity L_{151} against redshift z for the combined sample of FRII sources. The $L_{151} - z$ plane has been binned and the percentage of quasars in each bin shown, along with the associated Poisson errors. The first thing to note is that there are very few quasars at $\log_{10}(L_{151}/\text{W Hz}^{-1} \text{sr}^{-1}) < 26.5$. Excluding this region, the quasar fraction appears to increase slightly as a function of both redshift and radio luminosity, ranging from 0.3 to 0.5. However, with Poisson errors of $\sigma \sim 0.08$ these differences can at best be called marginally-significant, and we will not consider them further. Note also that for the high-luminosity bins, the median luminosity in

each bin changes with redshift, so the effects of redshift and luminosity have not been completely separated.

Laing et al. (1994) proposed that by excluding low-excitation radio galaxies (LEGs; Hine & Longair 1979) which have very weak or absent emission lines and low-ionization narrow lines, the quasar fraction in 3CRR was not a function of luminosity (or redshift). Their classification for LEGs was that they have [OIII] to H α ratios of < 0.2 and [OIII] equivalent widths of < 3 Å. Since the radio galaxies in the combined samples here span a large range of redshift, Balmer and/or [OIII] lines are often not observed in optical spectra and a classification scheme such as this cannot be applied. Instead we separate sources into those with high and low [OII] emission line luminosities. The division between these classes we adopt is $\log_{10}(L_{\text{[OII]}}/W) = 35.1$. Below this line luminosity there are very few broad line objects in the complete samples (Willott et al. 1999). This cut in narrow emission line luminosity was chosen to be equivalent to a rest-frame [OII] equivalent width of 10 Å for a quasar with $M_B = -23$ [†]. Note that this division puts more sources in the low-luminosity category than those typically classified as LEGs.

On the right-hand side of Fig. 1 we plot only sources with [OII] luminosities $\log_{10}(L_{\text{[OII]}}/W) \geq 35.1$. The differences between the quasar fractions in the bins is reduced somewhat here. Now we find that (with the exception of the poorly-populated low radio luminosity bin) the quasar fraction is 0.40 in all the bins at the 1σ level. The largest change has occurred in the low-redshift, intermediate luminosity bin which contains many weak-lined 3CRR galaxies. Note that the $1 \leq z < 2$, intermediate luminosity bin has the lowest quasar fraction. A possible reason for this is that this bin contains most of the galaxies without lines in their optical spectra which may not all truly lie within this redshift range. Considering all 216 high emission line luminosity sources plotted on the right-hand side of Fig. 1, we find a quasar fraction of 0.40 ± 0.03 implying a mean torus half-opening angle of $53^\circ \pm 3^\circ$ for the luminous population. There is likely to be quite a range of torus opening angles and the small error presented here on the mean angle should not be interpreted as the dispersion in opening angles present in the population.

We have repeated the analysis of this section excluding CSO sources (projected linear sizes ≤ 30 kpc). We find that this reduces the quasar fraction by ≈ 0.04 in all the bins. The quasar fraction of all luminous CSO sources is 0.56 ± 0.08 , different at the 2σ level from that of non-CSO sources. We defer discussion of possible reasons for a higher quasar

[†] The mean rest-frame equivalent width of the [OIII] line for BQs quasars in the study of Miller et al. (1992) is 30 Å. Assuming a ratio of 3:1 for the [OIII]:[OII] equivalent widths, this translates to 10 Å for [OII]. This value was used in Willott et al. (1999) to determine the strength of the photoionizing continuum in radio sources. However, the typical ratio between [OII] and [OIII] may actually be smaller than this, causing Willott et al to have overestimated the mean [OII] equivalent width by a factor of a few. Baker et al. (1999) finds a median [OII] equivalent width of 4 Å in the Molongo Quasar Sample. Also, in the LBQS composite quasar spectrum of Francis et al. (1991) the [OII] equivalent width is 2 Å, which would give a line luminosity of $\log_{10} L_{\text{[OII]}} = 35.1$ for a $M_B = -25$ quasar.

fraction for CSOs in low-frequency selected samples to a future paper.

4 POSSIBLE CAUSES OF THE CHANGE IN QUASAR FRACTION WITH LUMINOSITY

4.1 Selection effects caused by lower intrinsic broad line luminosity

We first investigate whether the decrease in quasar fraction with decreasing narrow-line and radio luminosity is a simple selection effect. If the low-luminosity objects have lower luminosity narrow emission lines it is natural to expect that their broad line and continuum luminosities should be lower too (e.g. Miller et al. 1992). It follows that their spectra may on average have lower signal-to-noise and weak broad lines may be missed. Given the strong correlation between narrow-line and radio luminosities (e.g. Willott et al. 1999) this could explain the deficit of broad line objects at radio luminosities $\log_{10}(L_{151} / \text{W Hz}^{-1} \text{sr}^{-1}) < 26.5$, and also the apparent constancy of the quasar fraction for objects with luminous narrow lines discussed in Section 3.

To test whether selection effects such as these could cause the apparent lack of low-luminosity broad line objects, we first calculate the expected broad line fluxes of objects in the 3CRR and 7C samples as a function of luminosity. To do this we make use of the fact that the narrow emission line luminosities of radio galaxies and quasars are positively correlated with low-frequency radio luminosity as shown in Willott et al. (1999). This correlation has a slope of 0.79 ± 0.04 in the sense that $L_{\text{[OII]}} \propto L_{151}^{0.79}$ and is most likely due to a correlation between jet power and photoionizing continuum luminosity (Rawlings & Saunders 1991). Use of this relation enables one to estimate the narrow line [OII] luminosity for values of radio luminosity.

A similar correlation between the broad line luminosity and radio luminosity is expected to hold. There are several lines of evidence supporting this. First, radio luminosity is correlated with the optical continuum luminosity for steep-spectrum quasars (Serjeant et al. 1998) and quasars show little variation in broad line equivalent widths over a wide range of luminosity (e.g. Osmer & Shields 1999). Second, Celotti et al. (1997) have shown that broad line luminosities are correlated with the power in pc-scale jets in radio-loud quasars.

To determine the relationship between the strengths of narrow and broad lines in quasar/BLRG spectra, we adopt the line ratios from the composite quasar spectrum of Francis et al. (1991). Although this is from an optically-selected sample, we do not expect significant differences between the line ratios of radio-loud and radio-quiet quasars. This is borne out by a comparison with the Molonglo Quasar Sample of Baker & Hunstead (1995): repeating the analysis using their line ratios gives a virtually identical result.

We consider a range of radio luminosities and attach to each one typical redshifts at which sources of these luminosities are observed in both the 3CRR and 7C samples. The correlation between the [OII] line and radio luminosity is then used to determine typical [OII] luminosities at each value of radio luminosity. From the typical wavelength range covered by optical spectra (4000Å–8500Å), we find the strongest

$\log_{10} L_{151}$ (WHz $^{-1}$ sr $^{-1}$)	z_{3CRR}	z_{7C}	broad line (3CRR)	broad line (7C)
28.0	1.2	4.0	MgII	Ly α
27.5	0.60	2.6	MgII	Ly α
27.0	0.35	1.8	H β	CIV
26.5	0.20	1.0	H α	MgII
26.0	0.13	0.60	H α	MgII
25.5	0.06	0.35	H α	H β
25.0	0.04	0.20	H α	H α

Table 1. This table shows typical redshifts of sources from the 3CRR and 7C samples (columns 2 and 3) at various radio luminosities (column 1). Columns 4 and 5 show the strongest broad lines observable over the relevant optical wavelength ranges corresponding to these redshifts.

broad line observable at each redshift. The typical luminosities, redshifts and strongest broad lines are shown in Table 1. Finally, we use the ratio of broad to [OII] lines in Francis et al. (1991) to calculate the luminosity and hence flux of the strongest broad line expected at each luminosity-redshift pair.

There is considerable scatter in the relationship between narrow emission line luminosity and radio luminosity ($\sigma = 0.5$ dex). Extra scatter comes in due to the conversion from narrow to broad line luminosities. Therefore a total scatter of $1\sigma = 0.6$ dex was assumed to determine the fraction of objects with broad line fluxes significantly below the characteristic values.

Figure 2 shows the expected flux of the strongest broad line observable at each redshift as listed in Table 1 for both 3CRR and 7C. Also plotted are the actual data for the 7C-I and 7C-II quasars and BLRGs (Willott et al. 1998a) and all 3CRR quasars with $z < 0.86$ in the RA range 18–12 hr (all from Jackson & Browne 1991 except 3C 109 from Goodrich & Cohen 1992). In general points corresponding to 3CRR BLRGs are not plotted because only a few of their broad line fluxes are available in the literature, although a few points from Hill et al. (1996) are plotted to illustrate the discussion of Section 4.2. The quasars which are red(dened) [$\alpha_{\text{opt}} > 1$, where $f_{\nu} \propto \nu^{-\alpha_{\text{opt}}}$] are shown as open symbols on Fig. 2; again the 3CRR spectrophotometric dataset is too inhomogeneous for this to be done reliably for 3CRR sources. Note that very few quasars fall below the limits of the model error bars. Virtually all of those which do are reddened (the exception is 5C6.282 at $z \approx 2$, which has an unusual spectrum with very narrow Ly α ; see Willott et al. 1998a). The similarity of the predicted fluxes with those observed justifies the use of the line ratios and method described here.

The key point to note from Fig. 2 is that as one considers lower radio luminosities in each sample (i.e. lower redshifts), the expected broad line fluxes *increase*. Therefore, so long as the spectra of lower redshift sources have similar exposure times to those at higher redshift, the broad lines should be visible if they are there and unreddened. For the 3CRR sample the spectra are rather inhomogeneous and it is difficult to prove that this is the case (but note that the deficit of 3CRR sources is most marked at $z < 0.3$, where the H α line is covered by optical spectra and the expected broad H α fluxes are high). However, in the 7C sample, simi-

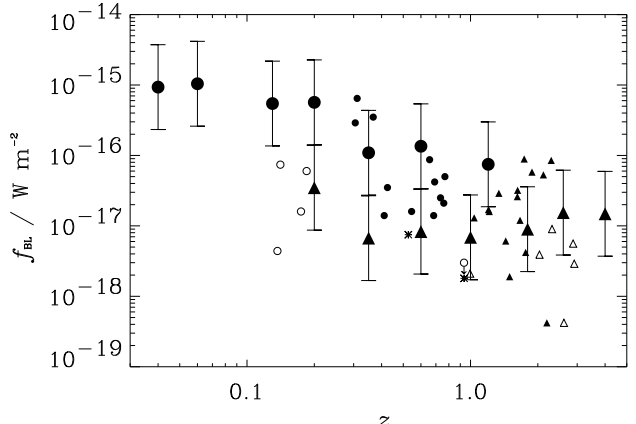


Figure 2. Expected broad line fluxes for ‘typical’ 3CRR (large circles) and 7C (large triangles) sources as a function of redshift according to the radio-optical correlation as described in Section 4.1. The error bars show approximate 1σ deviations (i.e. ≈ 1 in 6 sources should fall below the bottom of the error bars). The small symbols show the actual data for 3CRR (circles) and 7C (triangles) quasars and the 7C BLRGs (asterisks). Open triangles are 7C quasars which are known to be reddened. The open circles show the reddened quasar 3C 22 at $z = 0.93$ (broad MgII upper limit from Rawlings et al. 1995) and the 3C BLRGs from Hill et al. 1996 (see Section 4.2).

lar exposure times have been attained for the spectra at low redshift to those at high redshift. Therefore we are confident that in the absence of significant reddening of the BLR, an insignificant number of sources would be mis-classified.

A further problem is whether a weak quasar spectrum can be discerned against a stronger host galaxy spectrum. To determine if this could cause broad line selection problems, synthetic spectra of quasars and galaxies were created and combined. The model used for the galaxy spectra was a 1 Gyr old stellar population synthesis model of Bruzual & Charlot (1993). For the quasar spectra, the LBQS composite of Francis et al. (1991) was used. Poisson noise was added and it was found that broad H α or MgII should still be clearly visible for a quasar 2 magnitudes (in B -band) fainter than the galaxy (Fig. 3). Broad H β , however, is more difficult to detect. Spectra with poor blue wavelength coverage (e.g. no data below 5000 Å) of sources at $0.3 < z < 0.8$ would not include H α or MgII, in which case H β is the brightest line. Almost all the 7C and 6C spectra cover a large enough wavelength range to avoid this problem. However many spectra of 3CRR sources in the literature have a smaller wavelength range. But the radio-optical correlation (and Table 1) show that quasars at these redshifts in 3CRR typically have high luminosities and should not be fainter (at B -band) than their host galaxies. Indeed, the deficit of broad line objects in 3CRR only really begins at $z \lesssim 0.3$. Hence quasar broad lines should be clearly visible against typical background galaxy spectra down to $\log_{10}(L_{151} / \text{WHz}^{-1}\text{sr}^{-1}) \approx 25.5$, with possible problems only at fainter radio luminosities.

Another possibility to consider is that the narrow lines may be much stronger than the broad lines, so only weak wings in the line profiles would be seen. However, this picture seems unlikely for many sources in the absence of broad line reddening, since if both the narrow and broad lines are

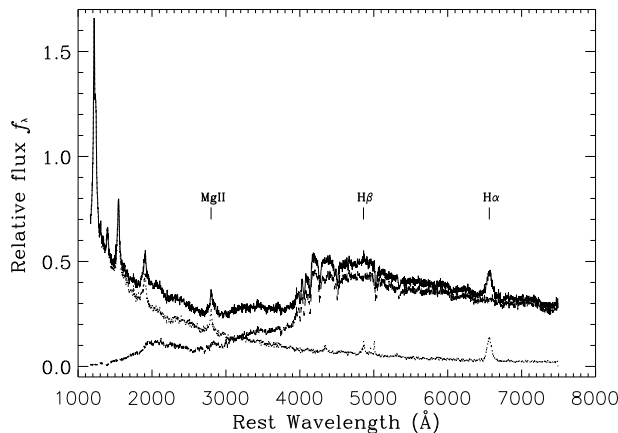


Figure 3. Superposition of a blue model quasar/BLRG spectrum and a red galaxy spectrum as described in the text. The quasar is two magnitudes fainter in B -band than the galaxy. The upper line shows the sum of the two components. Note that the broad MgII and H α lines are clearly visible in the total flux spectrum, the former because of the quasar dominance at wavelengths $\lambda < 3000 \text{ \AA}$ and the latter because of its high equivalent width.

photoionized by the same nuclear source it would require a conspiracy between broad and narrow line covering factors.

We conclude that the low quasar fraction at low luminosity is not due to selection effects caused by the difficulty of detecting intrinsically less luminous broad lines.

4.2 Increased reddening at low luminosities

In this section we consider the possibility that the drop in quasar fraction at low luminosities is due, at least in part, to an increase in the fraction of lightly-reddened ($0 \lesssim A_V \lesssim 5$) lines-of-sight as quasar luminosity decreases. It can be seen from Fig. 2 that the majority of the 7C quasars are lightly reddened at the highest redshifts. We exclude from this paper any discussion of any systematic changes of quasar reddening with cosmic epoch.

The question of the range of reddening towards the nuclei of powerful (3CRR) $z \sim 1$ radio sources has recently been addressed by the $3.5\mu\text{m}$ imaging programmes of Simpson, Rawlings & Lacy (1999) and Simpson & Rawlings (2000). They concluded that these high luminosity nuclei are mostly either naked ($A_V \sim 0$) or heavily obscured ($A_V \gtrsim 15$) with only a small fraction (~ 15 per cent) of intermediate lightly-reddened cases. If these results could be extrapolated to the lower narrow-line and radio luminosity regimes then light reddening of quasar nuclei would not be a serious issue for our study of the quasar fraction.

However, two studies suggest that the fraction of lightly-reddened lines-of-sight might increase significantly at lower narrow-line and radio luminosities. First, Hill, Goodrich & DePoy (1996) studied the Pa α and H α lines in a complete sample of low redshift ($0.1 < z < 0.2$) 3CR sources, looking for evidence of reddened broad lines in radio galaxies. These objects lie near the top of lowest- L_{151} (and z) bin in Fig. 1. They found broad lines in six objects out of a complete sample of thirteen (including two FRI sources), of which three had intermediate values of A_V .

This study, although subject to a major problem with small number statistics together with the difficulties of detecting lightly reddened broad lines over certain ranges of redshift (see Fig. 2), hints that an increase in the fraction of the lightly-reddened population at low luminosities might provide part of the explanation for the dropping quasar fraction at low luminosities. Second, Baker (1997) showed that a typical low-luminosity lobe-dominated quasar, i.e. an object akin to those near the top of lowest- L_{151} (and z) bin in Fig. 1, has a reddening $A_V \sim 3$ and is thus lightly reddened.

We conclude that some of the drop in the quasar fraction at low luminosities might be explained by an increased chance of light reddening towards low luminosity quasar nuclei. In other words, we cannot allay the suspicion that some lightly reddened quasars have been misclassified as galaxies on the basis of existing, chiefly optical, spectroscopy. In the lowest- L_{151} and z bin of Fig. 1 this is a problem for (very low- z) 3CRR sources because of the inhomogenous optical dataset; it is a problem for the 6C and 7C sources because their redshifts are sufficient to remove the strong H α line from the optical window (see Fig. 2). To pursue this idea further we next consider specific physical models which might explain this behaviour.

4.3 The receding torus model

Lawrence (1991) proposed that the apparent increase in quasar fraction and hence θ_{trans} with luminosity in the 3CRR sample could be explained naturally by a ‘receding torus’ model. Dust sublimates at $T \sim 1500 \text{ K}$ and therefore the inner radius of a dusty torus/disc may be governed by the radius at which this temperature is achieved via radiation from the AGN. The more luminous the AGN the larger this radius and if the scale height of the torus h is independent of luminosity, then more luminous sources will have a larger θ_{trans} ; the inner radius of the torus r scales as $L^{0.5}$ and $\theta_{\text{trans}} = \tan^{-1}(r/h)$. This model can also explain more lightly-reddened quasars at low luminosity since a larger fraction of the lines-of-sight pass through intermediate columns of obscuring material when the inner wall of the torus lies closer to the nucleus (see e.g. Fig. 8 of Hill et al. 1996).

Simpson (1998) has shown that if the height of the torus is independent of the ionizing luminosity L then the receding torus model predicts a theoretical quasar fraction f_q given by

$$f_q = 1 - \left(1 + \frac{L}{L_0} \tan^2 \theta_0 \right)^{-0.5}, \quad (1)$$

where L_0 and θ_0 are the normalisation luminosity and the torus half-opening angle at that luminosity, both of which are fixed by the measurement of the quasar fraction at some normalisation luminosity. We further assume that the [OII] luminosity scales with the ionizing continuum luminosity, and that it is not significantly affected by the changing torus opening angle, so that we can replace ionising luminosities in Eqn 1 by values of $L_{[\text{OII}]}$.[†] Binning all FRII sources in

[†] As emphasised by Simpson, [OII] is probably a far from ideal choice of narrow emission line for this procedure because for an ionisation-bounded emission line cloud, the [OII] emission is from

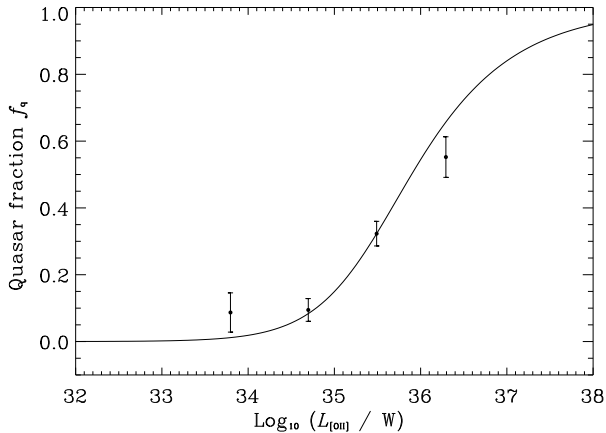


Figure 4. The points with Poisson error bars show the quasar fractions in four bins of [OIII] emission line luminosity plotted against the median $\log_{10}(L_{\text{[OIII]}})$ of the sources in each bin. The data used were for the objects deemed FRIIs in the combined sample 3CRR, 6C and 7C dataset (see Willott et al. 1999). The line is a simple prediction made on the basis of the receding torus model, normalised at $\log_{10}(L_{\text{[OIII]}}/W) = 35.5$, as described in Section 4.3.

terms of $L_{\text{[OIII]}}$ we find that for $35 < \log_{10}(L_{\text{[OIII]}}/W) < 36$, the quasar fraction is 0.32 ± 0.04 giving $\theta_0 = 46^\circ$. This is used to normalise Equation 1 which is plotted in Fig. 4 along with the quasar fraction measured in four bins of $\log_{10}(L_{\text{[OIII]}})$.

This simple model appears to fit the data fairly well although it does predict a marginally sharper transition between low and high quasar fractions than the data (at about the 1σ level). Note that the above model depends crucially upon the height of the torus being independent of luminosity. If the height of the torus increases with luminosity, albeit more slowly than the inner radius, then this would flatten the model distribution to something more closely resembling the data.

Taken together with the results of Hill et al. (1996), we conclude that the receding torus model provides a plausible if non-unique explanation for the declining quasar fraction below $\log_{10}(L_{\text{[OIII]}}/W) = 35.1$.

4.4 Dust-ejection by jets or outflow

Tadhunter et al. (1999) have recently obtained high-resolution near-infrared imaging of the powerful radio galaxy Cygnus A which shows an edge-brightened biconical structure roughly aligned with the jets. They suggest that at least some of the very high reddening towards the nucleus of Cygnus A ($A_V \approx 70$ mag) occurs in a kiloparsec scale dust-lane. For radio-loud sources, the jets may clear a path

a region whose size depends much less strongly on the incident photoionising flux than the sizes of the regions responsible for higher-ionization lines like [OIII]. This leads to a much weaker dependence of [OII] luminosity on incident photoionising luminosity L than the near proportionality between, say, [OIII] luminosity and L . Unfortunately, the choice of [OII] was forced on us by the available spectrophotometric data (see Willott et al. 1999).

through this dust, so that only when viewed within a critical angle of the jet-axis is there a chance of a line-of-sight having little reddening. The jet power could control the dust-clearing efficiency in such a way as to give an anti-correlation between reddening and radio luminosity. The conceptual difference between this model and the receding torus model is that it is now a decrease in jet power (and hence the radio luminosity) rather than a decrease in optical luminosity that controls the closing down of the effective opening angle of the radiation cone at low luminosities. Tadhunter et al. speculate that lightly reddened quasars are objects viewed within the nuclear torus opening angle, but not within the region cleared of dust by the jets. Another possibility (e.g. Dopita et al. 1998) is that dust is cleared by a radiation-driven outflow in which the opening angle and strength of the outflow could be related to the luminosity of the nucleus and hence give rise to the observed dependence of quasar fraction on luminosity.

4.5 Dual-population models

The evidence of increased reddening at low luminosities (Section 4.2) and the quantitative success of the receding torus model (Section 4.3) hint that we have a reasonable explanation for at least part of the drop in quasar fraction at low luminosities. In this section we discuss separate evidence for a second conceptually different mechanism.

A corollary of Fig. 4 is that at low luminosities the low fraction of quasars results from a small value for the typical opening angle of the torus θ_{trans} . Falcke et al. (1995) have cited this as a strength of the receding torus model since if the opening angle approaches the beaming angle of the jet then there will be an unobscured view of the nucleus of low power jets only when their emission is also strongly Doppler-boosted. Such objects would be classified as BL Lac objects rather than quasars, providing a neat explanation for the well-known lack of quasars with FRI radio structures. We are unaware of any systematic measurements of broad line fluxes in BL Lac type objects which would provide a quantitative test of this hypothesis. However, recent observations of BL Lacertae itself (Corbett et al. 2000), an object with an extended radio flux characteristic of a low-luminosity radio galaxy (Antonucci & Ulvestad 1985), suggest that in at least this object there are broad emission lines at about the predicted level, and that these lines are excited by a hot accretion disc.

However, other recent results suggest that the small opening angles required at low luminosities from Fig. 4 are more likely to argue against the generality of the receding torus model. If it were true that low luminosity radio galaxies possessed very thick obscuring tori then it should prove very difficult to get a clear view of their central regions at optical wavelengths. Chiaberge, Capetti & Celotti (1999) have studied the nuclear emission from FRI galaxies using the HST. In most cases they find probable optical synchrotron from the nuclear regions, which they interpret as implying a clear view of the inner jet and hence a lack of obscuring material on scales greater than ~ 100 pc. This straightforwardly rules out a kpc-scale obscuration model for FRIs along the lines of the model proposed by Tadhunter et al. (1999) for Cyg A. Still stronger constraints come from the nearby FRI radio galaxy M87 since its optical synchrotron

core is smaller than ~ 5 pc and varies on the timescales of months (Tsvetanov, Kriss & Ford 1997), implying that the emission region is a pc or smaller in size. Since the inner regions of the optical synchrotron-emitting jet are in clear view, and these size scales are comparable in size to the expected size of the obscuring torus in low-luminosity quasars (e.g. Netzer & Laor 1993), these results begin to question the existence of any thick torus, at least in the case of M87. Chiaberge et al. make stronger statements than this by making the additional assumption that this optical emission is emitted from within the region probed by radio VLBI which is argued to be within ~ 0.1 pc of the central black hole (Junor, Biretta & Livio 1999). We remain to be convinced that these observations rule out the existence of a pc-scaled torus in M87. There is a plethora of evidence from studies of M87 using optical continuum (Chiaberge et al. 1999), emission-line (Ford et al. 1994) and hard X-ray (Guainazzi & Molendi 1999) observations that it contains a supermassive black hole accreting at a tiny ($< 10^{-4}$) fraction of its Eddington-limited rate (see Willott et al. 1999 for a discussion of this object in the context of the radio-optical correlation).

As shown in Fig. 1, excluding objects with weak narrow emission lines gives a quasar fraction which is virtually independent of redshift and/or radio luminosity. This observation can be naturally explained if the weak-line objects belong to a different population from the strong emission line objects. Perhaps, as is seemingly the case for M87, a large fraction of these objects are fundamentally different in that they lack a well-fed quasar nucleus and also a thick obscuring torus (Chiaberge et al. 1999), and perhaps their jets are powered by a fundamentally different mechanism (e.g. Blandford & Begelman 1999). The continuity of the radio-optical correlation for radio sources provides a weak argument against a fundamental change in the accretion process (Rawlings & Saunders 1991), but evidence for systematic changes in the slope of this relation at low luminosities (Zirbel & Baum 1995) may be evidence that there are at least some differences at low radio luminosities. Arguing along similar lines, Laing et al. (1994) proposed that the low-excitation radio galaxies (LEGs) in their 3CRR sample would lack broad lines if viewed from any orientation. Recall that we specifically excluded FRI radio sources from our analysis of the quasar fraction in Section 3. The only difference that including the FRIs would have made, would be to decrease the quasar fraction in the lowest luminosity bin from 0.14 ± 0.04 to 0.10 ± 0.03 .

Such a ‘two population’ model would remove another troubling problem for any extrapolation of the receding torus model to the lowest quasar luminosities. Seyfert galaxies – radio-quiet AGN with similar optical narrow-line luminosities to radio galaxies in the lowest- L_{151} bin of Fig. 4 – do not have the narrow opening angles predicted by the receding torus model. Direct observations of the ionization cones in nearby Seyfert galaxies typically show cones with half-opening angles in the range $20 - 50^\circ$ (Wilson & Tsvetanov 1994), considerably greater than those predicted. Moreover, the vast majority of Seyfert galaxies do not seem to be obscured, i.e. of type 2, as would be required by narrow opening angles. Hence, as noted by Falcke et al. (1995) it would appear that the receding torus model cannot apply similarly to radio-quiet and radio-loud AGN requiring

some ad-hoc explanation, for example a different geometry for the obscuring material (i.e. a smaller scale height), due to a difference in black hole mass, environment and/or angular momentum.

We can make a crude association of the putative second population of radio sources with all sources with narrow emission line luminosities $\log_{10}(L_{\text{[OII]}}/\text{W}) < 35.1$. Due to the scatter in the radio-optical correlation, it is not expected that this would lead to a clean division between the two populations at a particular [OII] luminosity, and if the data were available, a classification based on line ratios, and hence excitation, might well prove cleaner. However, subject to this limitation, the change in quasar fraction with redshift of a combination of the two populations (seen on the left plot of Fig. 1) is then naturally explained by the less rapid cosmic evolution of the low-luminosity population (e.g. Urry & Padovani 1995) than the high-luminosity population (shown on the right plot of Fig. 1). Hence at high-redshift, the contribution of the low-luminosity population is negligible and the quasar fraction of 0.4 is just that of the high-luminosity population. Dual population modelling of the low-frequency radio luminosity function is consistent with just such a scheme (Jackson & Wall 1999; Willott et al. in prep.). Also, Laing et al. (1994) and Hardcastle et al. (1998) find that low-excitation radio galaxies have linear size and core prominence distributions consistent with an isotropic population.

There are two residual concerns with the two population model. First, many of the low-luminosity objects have emission lines, so their excitation and the correlation between luminosity and ionization parameter (Saunders et al. 1989; Tadhunter et al. 1998) need some explanation. Second, it must explain why radio galaxies and quasars have different narrow line luminosity distributions at intermediate luminosities (Jackson & Browne 1990) but similar distributions at high luminosities (Jackson & Rawlings 1997). The first concern can be addressed by simple analogy with M87: the absence of a broad-line quasar nucleus does not mean an absence of a photoionising source; for example Dopita et al. (1997) favour radiative shocks as a source of the excitation for the H α lines in the nuclear disc of M87, and shock models in which ionization parameter correlates with line luminosity are easily envisaged (e.g. Dopita & Sutherland 1995). The second concern is probably also easily dealt with. Considering first the 3CRR sample, the dual-population model is consistent with the drop in quasar fraction at low luminosities because a low luminosity 3CRR source is necessarily at low redshift where there is clearly a mixture of both populations; at high redshifts only the high-luminosity population is observed. Thus any comparative narrow emission line study of quasars and radio galaxies which is based on bright radio samples (Jackson & Browne 1990; Jackson & Rawlings 1997) should yield different line luminosity distributions at low redshift, and similar distributions at high redshift, which is just as observed. However, a small difference in the distributions of the [OII] line luminosities of intermediate luminosity quasars and radio galaxies is also observed in the 7C sample (Willott et al. 1999). The lower radio flux limit of this sample means that these intermediate luminosity sources are at high redshift, where there are few low emission line luminosity objects, so the difference is not due to the mixing of the two populations. This is most likely

the result of small but inevitable biases pointed out by Rawlings & Saunders (1991), and quantified in the context of the receding torus model by Simpson (1998): a positive correlation between quasar luminosity and opening angle, coupled with inevitable scatter in quasar luminosity at a fixed radio luminosity, means that objects viewed within the opening angle are biased towards the more luminous objects within the scatter.

4.6 Time variability

There is yet one more possible cause of the drop in quasar fraction at low luminosities: systematic differences in the time variability of objects with luminosity.

In Willott et al. (1999) we used the narrow emission line–radio correlation to suggest that the most luminous objects are probably accreting at rates close to the Eddington limit, but lower luminosity sources are sub-Eddington accreters. It therefore seems plausible that the lower luminosity sources have more scope for variability, since an object accreting at the Eddington rate should have a ready fuel supply which is accreted at a fairly steady rate limited by radiation pressure. In contrast, sub-Eddington accretion suggests there is not a ready supply of fuel available and hence fluctuations in accretion rate may be more likely. Indeed observations of radio-quiet quasars show that the lower luminosity quasars are more highly optically-variable than higher luminosity quasars over timescales of a few years (e.g. Véron & Hawkins 1995; Cristiani et al. 1996; Paltani & Courvoisier 1997), although it should be noted that some authors attribute at least some of this variability to gravitational microlensing (e.g. Hawkins & Taylor 1997).

The small quasar fraction at low luminosities could be explained by these objects spending a significant fraction of their active lifetimes in a ‘quiet’ state whereas the more luminous objects are continuously active over their entire lifetime. Due to light travel time effects, different emission regions of quasars have different variability timescales: BLR \sim months; NLR $\sim 10^4$ yr; radio lobes $\sim 10^6$ yr. Reverberation mapping of quasars has shown that the broad line fluxes follow the nuclear continuum flux with just such a time lag (see Peterson 1993 for a review). If a quasar undergoes high-amplitude variability over a timescale ~ 100 yr, then only the continuum and BLR fluxes would be observed to undergo this strong variability, and the NLR and extended radio emission would simply reflect the time-averaged output of the central engine. Note that a quasar undergoing a *decrease* in luminosity of this sort of timescale may then appear as a low-excitation radio galaxy. If this behaviour occurs only in a significant fraction of the intermediate and low luminosity objects, then it could reproduce the observed change in quasar fraction.

Essentially this model is a slightly more complicated version of the two-population model considered in Section 4.5, with the two populations being unified along a time rather than a jet orientation axis. It is important to stress that there is as yet no firm evidence for the type of time variability required. However, the few long-term time variability studies hint that there may be some interesting effects: the BLRG 3C 390.3 was found to undergo a sustained decrease of 1.5 mags in the optical over ≈ 80 years (Canion, Penston & Penston 1968); however, Angione (1973)

used archival plates to study the variability of 23 quasars over ≈ 60 years finding no evidence for long-term sustained increases or decreases.

A separate issue related to time variability is whether the probability of individual radio sources being observed to be quasars varies systematically throughout their lifetimes. Because flux-limited samples introduce inevitable biases into the age distributions of the sources they contain (e.g. Blundell, Rawlings & Willott 1999), this can lead to subtle effects.

5 CONCLUSIONS

Using complete, low-frequency selected samples of radio-loud AGN we have investigated the fraction of observed broad line objects – the quasar fraction – as a function of redshift, and radio and emission line luminosity. Our findings are interpreted in terms of orientation-based unified schemes. We find that

- Considering only those sources with strong narrow emission lines [$\log_{10}(L_{\text{[OIII]}}/\text{W}) \geq 35.1$, corresponding roughly to $\log_{10}(L_{151}/\text{W}) \geq 26.5$], the quasar fraction is virtually independent of radio luminosity and redshift, and is consistent with a simple unified scheme involving an obscuring torus with a half-opening angle θ_{trans} of 53° .
- For less luminous emission-line sources, the quasar fraction is much lower, a finding which is not simply the result of selection effects induced by the lower intrinsic broad line luminosities of these sources.

We have found evidence which supports at least two probable physical causes for the drop in quasar fraction at low luminosity: (i) a gradual decrease in θ_{trans} and/or a gradual increase in the fraction of lightly-reddened ($0 \lesssim A_V \lesssim 5$) lines-of-sight with decreasing quasar luminosity; and (ii) the emergence of a second population of low luminosity radio sources which, like M87, lack a well-fed quasar nucleus, and may well lack a thick obscuring torus.

ACKNOWLEDGEMENTS

We would like to thank Steve Eales, Gary Hill, Julia Riley and David Rossitter for important contributions to the 7C Redshift Survey. Thanks also to Robert Laing and Chris Simpson for some very useful discussions, and to the referee Ian Browne for useful suggestions. This research has made use of the NASA/IPAC Extra-galactic Database, which is operated by the Jet Propulsion Laboratory, Caltech, under contract with the National Aeronautics and Space Administration. CJW thanks PPARC for support.

REFERENCES

Angione R.J., 1973, AJ, 78, 353
Antonucci R.R.J., 1993, ARAA, 31, 473
Antonucci R.R.J., Ulvestad J.S., 1985, ApJ, 294, 158
Baker J.C., 1997, MNRAS, 286, 23
Baker J.C., Hunstead R.W., 1995, ApJ, 452, L95
Baker J.C., Hunstead R.W., Kapahi V.K., Subrahmanya C.R., 1999, ApJS, 122, 29

Barthel P.D., 1989, *ApJ*, 336, 606

Baum S.A., Heckman T.M., 1989, *ApJ*, 336, 702

Blandford R.D., Begelman M.C., 1999, *MNRAS*, 303, L1

Blundell K.M., Rawlings S., Willott C.J., 1999, *AJ*, 117, 677

Browne I.W.A., Jackson N., 1992, in Duschl. W., Wagner., eds, Physics of Active Galactic Nuclei. Springer, Berlin. p.61

Bruzual G., Charlot S., 1993, *ApJ*, 405, 538

Cannon R.D., Penston M.V., Penston M.J., 1968, *Nature*, 217, 340

Celotti A., Padovani P., Ghisellini G., 1997, *MNRAS*, 286, 415

Chiaberge M., Capetti A., Celotti A., 1999, *A&A*, 349, 77

Cristiani S., Trentini S., La Franca F., Arétxaga I., Andreani P., Vio R., Gemmo A., 1996, *A&A*, 306, 395

Corbett E.A., Robinson A., Axon D.J., Hough J.H., 2000, *MNRAS*, 311, 485

Dopita M.A., Sutherland R.S., 1995, *ApJ*, 455, 468

Dopita M.A., Koratkar A.P., Allen M.G., Tsvetanov Z.I., Ford H.C., Bicknell G.V., Sutherland R.S., 1997, *ApJ*, 490, 202

Dopita M.A., Heisler C., Lumsden S., Bailey J., 1998, *ApJ*, 498, 570

Eales S.A., 1985, *MNRAS*, 217, 149

Falcke H., Gopal-Krishna, Biermann P.L., 1995, *A&A*, 298, 395

Ford H.C., Harms R.J., Tsvetanov Z.I., Hartig G.F., Dressel L.L., Kriss G.A., Bohlin R.C., Davidsen A.F., Margon B., Kochhar A.K., 1994, *ApJ*, 435L, 27

Francis P.J., Hewett P.C., Foltz C.B., Chaffee F.H., Weymann R.J., Morris S.L., 1991, *ApJ*, 373, 465

Goodrich R.W., Cohen M.H., 1992, *ApJ*, 391, 623

Guainazzi M., Molendi S., 1999, *A&A*, 351L, 19

Hardcastle M.J., Alexander P., Pooley G.G., Riley J.M., 1998, *MNRAS*, 296, 445

Hawkins M.R.S., Taylor A.N., 1997, *ApJ*, 482, 5

Hes R., Barthel P.D., Fosbury R.A.E., 1996, *A&A*, 313, 423

Hill G.J., Goodrich R.W., DePoy D.L., 1996, *ApJ*, 462, 163

Hine R.G., Longair M.S., 1979, *MNRAS*, 188, 111

Jackson C.A., Wall J.V., 1999, *MNRAS*, 304, 160

Jackson N., Browne I.W.A., 1990, *Nature*, 343, 43

Jackson N., Browne I.W.A., 1991, *MNRAS*, 250, 414

Jackson N., Rawlings S., 1997, *MNRAS*, 286, 241

Junor W., Biretta J.A., Livio M., 1999, *Nature*, 401, 891

Lacy M., Rawlings S., Hill G.J., Bunker A.J., Ridgway S.E., Stern D., 1999, *MNRAS*, 308, 1096

Laing R.A., Riley J.M., Longair M.S., 1983, *MNRAS*, 204, 151

Laing R.A., Jenkins C.R., Wall J.V., Unger S.W., 1994, in Bicknell G., ed., Proceedings of the Stromlo Centenary Symposium: Physics of Active Galactic Nuclei. Springer-Verlag, Berlin, p.201

Lawrence A., 1991, *MNRAS*, 252, 586

McCarthy P.J., Spinrad H., van Breugel W., 1995, *ApJS*, 99, 27

Miller P., Rawlings S., Saunders R., Eales S.A., 1992, *MNRAS*, 254, 93

Netzer H., Laor A., 1993, *ApJ*, 404L, 51

Osmor P.S., Shields J.C., 1999, in Ferland G., Baldwin J., eds., Quasars and Cosmology, ASP Conference Series 162, 235

Paltani S., Courvoisier T.J.-L., 1997, *A&A*, 323, 717

Peterson B.M., 1993, *PASP*, 105, 247

Rawlings S., Saunders R., 1991, *Nature*, 349, 138

Rawlings S., Saunders R., Eales S.A., Mackay C.D., 1989, *MNRAS*, 240, 701

Rawlings S., Lacy M., Sivia D.S., Eales S.A., 1995, *MNRAS*, 274, 428

Saunders R., Baldwin J.E., Rawlings S., Warner P.J., Miller L., 1989, *MNRAS*, 238, 777

Scheuer P.A.G., 1987, in *Superluminal Radio Sources*, edited by J.A. Zensus and T.J. Pearson, p.331, Cambridge University Press

Serjeant S., Rawlings S., Maddox S.J., Baker J.C., Clements D., Lacy M., Lilje P.B., 1998, *MNRAS*, 294, 494

Simpson C., 1998, *MNRAS*, 297, L39

Simpson C., Rawlings S., 2000, *MNRAS*, submitted

Simpson C., Rawlings S., Lacy M., 1999, *MNRAS*, 306, 828

Singal A.K., 1993, *MNRAS*, 262, L27

Singal A.K., 1996, *MNRAS*, 278, 1069

Tadhunter C.N., Morganti R., Robinson A., Dickson R., Villar-Martin M., Fosbury R.A.E., 1998, *MNRAS*, 298, 1035

Tadhunter C.N., Packham C., Axon D.J., Jackson N.J., Hough J.H., Robinson A., Young S., Sparks W., 1999, *ApJ*, 512, L91

Tsvetanov Z.I., Kriss G.A., Ford H.C., 1997, *AAS*, 191, 130.02

Urry C.M., Padovani P., 1995, *PASP*, 107, 803

Véron P., Hawkins M.R.S., 1995, *A&A*, 296, 665

Willott C.J., Rawlings S., Blundell K.M., Lacy M., 1998a, *MNRAS*, 300, 625

Willott C.J., Rawlings S., Blundell K.M., Lacy M., 1998b, in Observational Cosmology with the New Radio Surveys, eds. M.N. Bremer et al., 209, Kluwer

Willott C.J., Rawlings S., Blundell K.M., Lacy M., 1999, *MNRAS*, 309, 1017

Wilson A.S., Tsvetanov Z.I., 1994, *AJ*, 107, 1227

Zirbel E.L., Baum S.A., 1995, *ApJ*, 448, 521